

AD-A186 236

HIGHER HARMONIC GENERATION IN THE INDUCED RESONANCE  
ELECTRON CYCLOTRON MR. (U) SCIENCE APPLICATIONS  
INTERNATIONAL CORP MCLEAN VA 5 RYKOPOULOS ET AL.

141

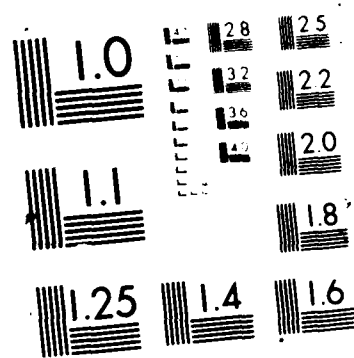
UNCLASSIFIED

SEP 87 NRL-MR-6072 DE-A105-83ER40117

F/G 9/3

44

Figure 1 displays a 3x13 grid of plots. The first 12 columns show the spatial distribution of the system at different times, with the first column being the initial state and the subsequent columns showing the development of a wave. The 13th column shows the time evolution of the total energy, with the top row labeled  $E$ , the middle row labeled  $E/N$ , and the bottom row labeled  $E/N^2$ .





**NRL Memorandum Report 6072**

**AD-A186 236**

**Higher Harmonic Generation in the Induced Resonance  
Electron Cyclotron Maser**

**S. RIYOPOULOS,\* C. M. TANG, P. SPRANGLE AND B. LEVUSH†**

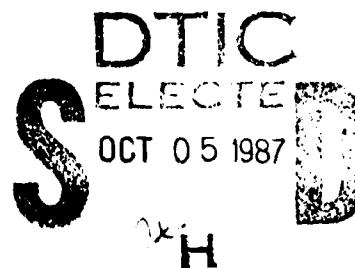
*Plasma Theory Branch  
Plasma Physics Division*

*\*Science Applications International Corp.  
McLean, VA 22102*

*†University of Maryland  
College Park, MD 20742*

**September 24, 1987**

**DTIC FILE COPY**



## REPORT DOCUMENTATION PAGE

1a. REPORT SECURITY CLASSIFICATION <b>UNCLASSIFIED</b>			1b. RESTRICTIVE MARKINGS		
2a. SECURITY CLASSIFICATION AUTHORITY			3. DISTRIBUTION / AVAILABILITY OF REPORT  Approved for public release; distribution unlimited.		
2b. DECLASSIFICATION / DOWNGRADING SCHEDULE					
4. PERFORMING ORGANIZATION REPORT NUMBER(S) NRL Memorandum Report 6072			5. MONITORING ORGANIZATION REPORT NUMBER(S)		
6a. NAME OF PERFORMING ORGANIZATION Naval Research Laboratory		6b. OFFICE SYMBOL (if applicable) Code 4790		7a. NAME OF MONITORING ORGANIZATION	
6c. ADDRESS (City, State, and ZIP Code) Washington, DC 20375-5000			7b. ADDRESS (City, State, and ZIP Code)		
8a. NAME OF FUNDING / SPONSORING ORGANIZATION U.S. Dept. of Energy		8b. OFFICE SYMBOL (if applicable)		9. PROCUREMENT INSTRUMENT IDENTIFICATION NUMBER J.O. #47-2005-0-6	
8c. ADDRESS (City, State, and ZIP Code) Washington, DC 20545			10. SOURCE OF FUNDING NUMBERS		
			PROGRAM ELEMENT NO. DOE	PROJECT NO. AJ05-83 ER40117	TASK NO. ORD (326)
			WORK UNIT ACCESSION NO. 380-537		
11. TITLE (Include Security Classification) Higher Harmonic Generation in the Induced Resonance Electron Cyclotron Maser					
12. PERSONAL AUTHOR(S) Riyopoulos, <sup>1</sup> S., Tang, C.M., Sprangle, P., and Levush, <sup>2</sup> B.					
13a. TYPE OF REPORT Interim		13b. TIME COVERED FROM _____ TO _____		14. DATE OF REPORT (Year, Month, Day) 1987 September	
15. PAGE COUNT 36					
16. SUPPLEMENTARY NOTATION <sup>1</sup> Science Applications Intl. Corp., McLean, VA 22102 <sup>2</sup> University of Maryland, College Park, MD 20742					
17. COSATI CODES			18. SUBJECT TERMS (Continue on reverse if necessary and identify by block number)		
FIELD	GROUP	SUB-GROUP	Masers		
			Gyrotrons		
			Radiation sources		
19. ABSTRACT (Continue on reverse if necessary and identify by block number)  The operation of the induced resonance electron cyclotron (IREC) maser at Doppler upshifted cyclotron harmonics is studied. A set of fast-time averaged nonlinear equations of motion is derived for the particle motion near an arbitrary harmonic at any index of refraction. The small signal efficiency is computed analytically and the minimum current to start the cavity oscillations is obtained. The nonlinear equations of motion are integrated numerically. The interaction efficiency at the first few harmonics is found comparable to the efficiency at the fundamental. The sensitivity of the efficiency to the beam thermal spreads is minimized by the proper selection of the index of refraction.					
20. DISTRIBUTION / AVAILABILITY OF ABSTRACT <input checked="" type="checkbox"/> UNCLASSIFIED/UNLIMITED <input type="checkbox"/> SAME AS RPT <input type="checkbox"/> DTIC USERS			21. ABSTRACT SECURITY CLASSIFICATION UNCLASSIFIED		
22a. NAME OF RESPONSIBLE INDIVIDUAL C. M. Tang			22b. TELEPHONE (Include Area Code) (202) 767-4148		22c. OFFICE SYMBOL Code 4791

## CONTENTS

I. INTRODUCTION .....	1
II. FIELD MODELING AND PARTICLE DYNAMICS .....	4
III. SMALL SIGNAL EFFICIENCY .....	8
IV. THERMAL EFFECTS .....	11
V. NUMERICAL RESULTS .....	13
ACKNOWLEDGMENT .....	15
REFERENCES .....	16



Accession For	
NTIS GFA&I	<input checked="" type="checkbox"/>
DTIC TAB	<input type="checkbox"/>
Unannounced	<input type="checkbox"/>
Justification	<input type="checkbox"/>
By	
Distribution	
Availability Codes	
Avail and	
Dist	Special

# HIGHER HARMONIC GENERATION IN THE INDUCED RESONANCE ELECTRON CYCLOTRON MASER

## I. INTRODUCTION

Generation of intense radiation in the microwave regime through electron cyclotron interaction was proposed independently by a number of researchers<sup>1-4</sup> in the late 1950s. Electrons gyrating in resonance with the radiation field experience a bunching in the relative wave particle phase through the dependence of the cyclotron frequency on the relativistic mass. High amplification of the radiation field, known as masing action, results for radiation frequencies slightly above the electron cyclotron frequency. Electron cyclotron masers<sup>5-18</sup>, also called gyrotrons, have demonstrated efficient high power generation capability at the centimeter wavelengths. Electron cyclotron instabilities also occur in ionospheric and astrophysic plasmas<sup>19,20</sup>.

A variety of potential applications, such as advanced accelerators, heating of fusion plasmas, short wavelength radar and spectroscopy, call for generation of intense radiation at even shorter wavelengths in the millimeter and submillimeter range. In a closed resonator, the shortest wavelength for single mode operation is tied to the transverse dimension of the cavity. Operation at radiation wavelengths shorter than the transverse dimensions will result in a multimode excitation<sup>21</sup> due to the small frequency separation among cavity eigenmodes. This limitation in the wavelength is considerably relaxed in the quasi-optical maser<sup>22,23</sup> operating in an open resonator that offers much improved frequency separation.

Considerable attention has been given lately to the operation at Doppler upshifted frequencies<sup>24-30</sup> resulting from a finite wave number  $k_z$  in the direction of the electron beam propagation. The operation frequency  $\omega$ , defined by the resonance condition  $\omega - k_z v - \Omega_c = 0$ , is given by

$$\omega = \Omega_c (1 - n_z \beta_z)^{-1},$$

where  $\gamma$  is the relativistic factor  $\gamma = (1 - \beta^2)^{-1/2}$ ,  $\beta = v/c$ ,  $n_z = k_z c / \omega$  is the parallel index of refraction and  $\Omega_c = \Omega_0 / \gamma$  is the relativistic cyclotron frequency with  $\Omega_0 = eB_0 / mc$ . For  $n_z = \beta_z = 1$  the frequency is boosted to  $2\gamma_z^2$  times the electron cyclotron frequency with  $\gamma_z = (1 - \beta_z^2)^{-1/2}$ . Note that both parallel and perpendicular kinetic energy of the electrons feed the instability in case of a tilted resonator. So far plane wave configurations in simple geometry, also referred to as the cyclotron autoresonance maser<sup>24</sup> (CARM), have been analyzed<sup>24-27</sup> in conjunction with Doppler upshifting of the radiation frequency.

The induced resonance electron cyclotron (IREC) maser<sup>28-31</sup>, shown in Fig. 1, operates at Doppler upshifted frequencies, utilizing at the same time the advantages of the open resonators. Each resonator forms an angle  $\alpha$  with the direction of the electron beam along the external magnetic field. The index of refraction  $n_z = \cos \alpha$  is adjustable by varying the angle between the resonators and can be chosen to minimize the effects of finite beam thermal spreads. For operation at the optimum refraction index the efficiency is relatively insensitive to the beam energy spread. The sensitivity to the beam pitch angle spread can also be minimized. The interaction length inside the resonator that maximizes efficiency is of the order of half a bounce distance<sup>14</sup> for the trapped particles.

As the available magnetic field limits the maximum operation frequency for given  $\gamma$ , operation at higher harmonics<sup>31,32</sup> becomes very attractive. The magnetic field required to produce radiation at a given frequency is reduced to a fraction  $1/(N + 1)$  for operation at the Nth harmonic. Operation at higher harmonics has been analyzed for the conventional<sup>33,34</sup> and quasioptical<sup>35,36</sup> gyrotron, showing that considerable efficiency can be

achieved at the first few harmonics. Previous IREC studies have considered operation at the fundamental frequency and small Larmor radius, relevant to the case of small resonator angle and small pitch angle  $\theta = v_{\perp}/v_z$ . In the present work we analyze operation at any given harmonic  $N$  and arbitrary resonator angle including finite Larmor radius effects. The effects of the Gaussian radiation profile are retained as well. A set of slow time scale equations of motion is derived by averaging over the cyclotron period time scale. The small signal efficiency is determined analytically. Nonlinear efficiency is determined by numerical integration. It is found that the efficiency for the first few harmonics is comparable to that for the fundamental in the same parameter regime. This is feasible because saturation occurs at larger radiation amplitude with higher harmonics. The effects of energy, pitch angle and guiding center spread are also studied. An optimum resonator angle  $\alpha$  exists for a given set of parameters minimizing the effects of finite beam thermal spreads. Efficiency enhancement can be achieved by properly tapering the external magnetic field<sup>29</sup>, inducing an extended wave particle resonance.

The remainder of this paper is organized as follows. In Section II, we describe the field in the resonator and we obtain the fast-time averaged equation of motion. In Section III, the small signal efficiency and the start-up current required to trigger the oscillations in the resonator are calculated. In Section IV, we discuss briefly the effects caused by the finite thermal spreads in the electron energy and pitch angle. In Section V, we integrate numerically the equations of motion using velocity distributions with finite energy and pitch angle spread as well as guiding center distribution in the transverse direction. The nonlinear efficiency is computed for the first few harmonics.



## II. FIELD MODELING AND PARTICLE DYNAMICS

The configuration for the induced resonance electron cyclotron (IREC) maser is shown schematically in Fig. 1. The interaction cavity is formed by the two quasi-optical resonators intersecting at an angle  $2\alpha$  where  $\alpha$  is the angle relative to the external magnetic field  $B_0$  along the  $z$ -axis. The electron beam also propagates along  $z$ . The total vector field is the superposition of the two resonant fields

$$A(x', y', z'; t)_{\alpha} + A(x', y', z'; t)_{-\alpha}, \quad (1)$$

where  $A(x', y', z'; t)$  are eigenmodes of the Fabry-Perot type resonator. Here we consider the lowest order Gaussian  $TEM_{00}$  modes linearly polarized along the  $y$ -axis

$$A(x', y', z'; t) = \hat{e}_y \frac{1}{4} A_0 \exp \left[ -i \left( \frac{k}{2} \frac{x'^2 + y'^2}{q(z')} - u(z') \right) \right] \left\{ \exp [i(kz' - \omega t)] + \exp [-i(kz' + \omega t)] \right\} + c.c., \quad (2)$$

where

$$\frac{1}{q(z')} = \frac{1}{R(z')} - i \frac{\lambda}{\pi w^2(z')}, \quad R(z') = z' \left[ 1 + \left( \frac{z'}{Z_0} \right)^2 \right],$$

$$w(z') = w_0 \left[ 1 + \left( \frac{z'}{Z_0} \right)^2 \right]^{1/2}, \quad u(z') = \tan^{-1} \left( \frac{z'}{Z_0} \right),$$

$w_0$  is the beam waist at the center of the resonator,  $\lambda$  is the wavelength and  $Z_0 = \pi w_0^2 / \lambda$  is the Rayleigh length.

The coordinates  $(x', y', z')_{\pm\alpha}$  have the  $z'$ -axis aligned with each resonator and are related to  $(x, y, z)$  by

$$\begin{pmatrix} x' \\ z' \end{pmatrix} = \begin{pmatrix} \cos\alpha & \pm\sin\alpha \\ \pm\sin\alpha & \cos\alpha \end{pmatrix} \begin{pmatrix} x \\ z \end{pmatrix}, \quad (3)$$

$$y' = y,$$

The radiation field is assumed at temporarily steady state. The Gaussian width  $w_0$  for the radiation envelope is much larger than the radiation wavelength  $\lambda$  and the beam spot size  $b$ . The Rayleigh length  $Z_0$  is typically much longer than the interaction length  $L \sim w_0/\sin\alpha$  in the  $z$ -direction. In the vicinity of the beam  $x \sim y \sim b$ , and within the interaction regime  $|z| \sim L$ , we have  $b/L \sim z/Z_0 \sim \epsilon \ll 1$ ,  $b/Z_0 \sim \epsilon^2$ . Combining Eqs. (1) - (3), and dropping terms of order  $\epsilon^2$ , the forward propagating component of the total field near the interaction area is expressed as

$$A_t(x, y, z; t) = \hat{e}_y A_0 e^{-\frac{z^2 \sin^2 \alpha}{w_0^2}} \cos k_\perp x \cos (k_z z - \omega t), \quad (4)$$

where  $k_\perp = (\omega/c) \sin \alpha$ ,  $k_z = (\omega/c) \cos \alpha$ .

In short, Gaussian effects in the transverse direction of order  $b^2/L^2 \sim \epsilon^2$  have been omitted while the electrons experience a Gaussian envelope of effective width  $L = w_0/\sin\alpha$  in the  $z$ -direction. Only the forward propagating wave phase is considered in Eq. (4) since the synchronous interaction of an electron with the backward component occurs at down-shifted cyclotron frequency, of small practical interest.

We use the guiding center description for the particle orbits

$$\begin{aligned} x &= x_g + \rho \sin \zeta, & y &= y_g - \rho \cos \zeta, \\ p_x &= p_{gx} + p_\perp \cos \zeta, & p_y &= p_{gy} + p_\perp \sin \zeta, \end{aligned} \quad (5)$$

with  $(x_g, y_g)$  and  $(p_{gx}, p_{gy})$  denoting the guiding center position and momentum,  $\rho$  is the Larmor radius,  $p_\perp$  is the magnitude of the transverse momentum and  $\zeta$  is the gyroangle. By averaging the exact Lorentz force equations in the vector potential representation over the fast (cyclotron)

time scale, the slow time scale nonlinear relativistic equations of motion are cast in the form

$$\frac{dx_g}{dz} = - \frac{\Delta\omega}{\Omega_0} \frac{\gamma}{u_z} a J_N(k_\perp \rho) \sin \psi_N \cos g_N, \quad (6a)$$

$$\frac{dy_g}{dz} = \frac{ck_\perp}{\Omega_0} \gamma \frac{u_\perp}{u_z} a J'_N(k_\perp \rho) \cos \psi_N \cos g_N, \quad (6b)$$

$$\frac{du_\perp}{dz} = \left( \frac{\gamma\omega}{cu_z} - k_z \right) a J'_N(k_\perp \rho) \sin \psi_N \sin g_N, \quad (6c)$$

$$\frac{du_z}{dz} = k_z \frac{u_\perp}{u_z} a J'_N(k_\perp \rho) \sin \psi_N \sin g_N, \quad (6d)$$

$$\begin{aligned} \frac{d\psi_N}{dz} = & - \frac{\gamma\Delta\omega}{cu_z} + \frac{N^2}{u_\perp} \left( \frac{\gamma\omega}{cu_z} - k_z \right) a \frac{J'_N(k_\perp \rho)}{k_\perp \rho} \cos \psi_N \sin g_N \\ & - N \frac{k_\perp}{u_z} a J_N(k_\perp \rho) \cos \psi_N \sin g_N. \end{aligned} \quad (6e)$$

In Eqs. (6a) to (6e) the prime (') signifies the Bessel function derivative in respect to the argument,  $u$  is the normalized momentum  $u = p/mc = \gamma v/c$ ,  $\gamma$  is the relativistic factor  $\gamma = (1 + u_\perp^2 + u_z^2)^{1/2}$ ,  $\psi_N = k_z z - \omega t + N\zeta + N\pi/2$  is the relative phase between the field and the particle,  $g_N = k_\perp x_g - N\pi/2$  carries the dependence on the guiding center position,  $a(z) = a_0 \exp(-z^2/L^2)$  is the normalized radiation amplitude with  $a_0 = eA_0/mc^2$  and the detuning in frequency  $\Delta\omega$  is given by

$$\Delta\omega = \omega(1 - n_z \beta_z) - N\Omega_0/\gamma. \quad (7)$$

It is the dependence of the detuning  $\Delta\omega$  on the particle energy through the relativistic correction  $\gamma$  that causes the phase bunching and the radiation

amplification in the linear regime. The evolution of  $\gamma$  is found combining Eqs. (6c) to (6e),

$$\frac{d\gamma}{dz} = \frac{\omega}{c} \frac{u_{\perp}}{u_z} a J'_N(k_{\perp} \rho) \sin \psi_N \sin g_N. \quad (8)$$

In performing the fast time averaging to obtain Eqs. (6)-(8) we have assumed that the particles always remain close to resonance with a single harmonic  $N$ , i.e.,  $\omega(1-n_z \beta_z) - N\Omega_0/\gamma \approx 0$ . Therefore the change in energy  $\Delta\gamma$  and consequently the radiation amplitude  $a_0$  cannot exceed a certain limit. When  $a_0$  is very large, the particles may also experience resonant effects from nearby harmonics  $N \pm 1$ . The validity conditions for a single resonant harmonic are satisfied in the parameter regime under consideration.

The nonlinear system of differential equations (6)-(8) cannot be solved analytically in terms of elementary functions, except in some special cases<sup>37,38</sup>. We resort to numerical integration in order to examine the nonlinear behavior while the small signal analysis is done by perturbation theory.

### III. SMALL SIGNAL EFFICIENCY

One of the issues concerning intense microwave generation is the intrinsic efficiency  $\eta$  of the interaction, defined as

$$\eta = - \frac{\langle \gamma_f - \gamma_o \rangle}{\langle \gamma_o - 1 \rangle} = - \langle \gamma_o - 1 \rangle^{-1} \int dp_o^3 f(p_o) \int dg_o \int d\psi_o \int_{-\infty}^{\infty} dz \frac{d\gamma}{dz}, \quad (9)$$

where  $\langle \rangle$  signifies the average over the initial distribution in phase space, and  $\gamma$  is a function of the initial conditions  $\gamma(z; p_{10}, p_{z0}, \psi_o, g_o)$  with  $\psi_o = \psi_N(-\infty)$  and  $g_o = g_N(-\infty)$ . We compute the small signal efficiency in order to determine the beam current required to overcome losses and start the cavity oscillations. After obtaining the linearized solutions of Eqs. (6) to (8), we substitute them into the integrant in the right-hand side of Eq. (9). The evaluation of the final result is considerably simplified by taking the phase space average over  $\psi_o$  before the spatial integration<sup>22,36</sup> over  $z$ . Expanding the products of trigonometric terms inside the integrant into sums, averaging over  $\psi_o$  and extending the limits of the  $z$ -integration to  $\pm\infty$ , we obtain the linear efficiency in terms of the initial conditions

$$\begin{aligned} \eta = & \frac{\pi}{4} \frac{a_o^2 \xi^2}{\gamma_o(\gamma_o - 1)} \left( J'_N(s_o) \right)^2 \exp \left( - \frac{1}{2} \xi^2 \frac{\Delta\omega_o^2}{\omega^2} \right) \langle \sin^2 g_o \rangle \\ & \left\{ \left( n_z \beta_{z0} - 1 \right) \left( 1 + \frac{N^2 J_N(s_o)}{s_o J'_N(s_o)} + \frac{s_o J''_N(s_o)}{J'_N(s_o)} \right) + \theta_o \beta_{z0} \left( \theta_o n_z + \frac{N J_N(s_o)}{J'_N(s_o)} n_{\perp} \right) \right. \\ & \left. + \left( \xi^2 \beta_{10}^2 (1 - n_z^2) - \frac{\langle \cos^2 g_o \rangle}{\langle \sin^2 g_o \rangle} \frac{s_o J_N(s_o)}{J'_N(s_o)} \right) \left( \frac{\Delta\omega_o}{\omega} \right) - n_z \beta_{z0} \theta_o^2 \xi^2 \left( \frac{\Delta\omega_o}{\omega} \right)^2 \right\}, \quad (10) \end{aligned}$$

where  $s_o = k_{\perp} p_o$ ,  $g_o = k_{\perp} x_{go} - N\pi/2$ ,  $\beta_{10} = v_{10}/c$ ,  $\beta_{z0} = v_{z0}/c$ ,  $\theta_o = v_{10}/v_{z0}$  and  $\langle f \rangle = (1/2\pi) \int_0^{2\pi} d(k_{\perp} x_g) f$  is the average over the initial guiding center position.

We have chosen to express  $\eta$  in terms of the parameters  $\Delta\omega_0/\omega$  and  $\xi = \omega\tau$ , where  $\tau = \gamma_0 L/cu_{z0}$  is the transit time through the interaction regime. The argument  $\xi\Delta\omega_0/\omega$  in the exponential is equal to  $\Delta\omega_0\tau$ , the linear advance in the relative phase  $\Delta\psi_0$  over the interaction regime. The sign is determined by the angular bracket on the right-hand side of Eq. (10). Treating the bracket as a quadratic form in  $\Delta\omega_0/\omega$  and keeping the lowest order contribution in  $k_{\perp}\rho$ , we find that the regime for positive efficiency is given approximately by

$$\frac{[(N+1)(1 - n_z\beta_{z0}) - \theta_0^2 n_z\beta_{z0}]}{(1 - n_z^2)\beta_{\perp 0}^2 \xi_0^2} < \frac{\Delta\omega_0}{\omega} < \frac{\beta_{\perp 0}^2(1 - n_z^2)}{n_z\beta_{z0}\theta_0^2}.$$

The upper limit in  $\Delta\omega_0/\omega$  is due to the finite  $n_z$  and results from the negative contribution of the quadratic term  $(\Delta\omega/\omega)^2$  that overtakes the positive contribution of the linear terms for small angle,

$$\sin^2\alpha < \frac{n_z\beta_{z0}\theta_0^2}{\beta_{\perp 0}^2} \frac{\Delta\omega_0}{\omega}.$$

For typical operation parameters we have  $\xi \gg 1$  and  $\Delta\omega_0/\omega \ll 1$ . In order to estimate the maximum efficiency within the positive regime, we parametrize Eq. (10) as a function of  $\zeta = \xi\Delta\omega_0/\omega$  and look for the zeros of the cubic equation resulting from  $d\eta/d\zeta = 0$ . If the angle  $\alpha$  is not too small,  $\sin^2\alpha \gg 1/\xi\beta_{\perp 0}^2$  where  $\xi \gg 1$ , then the maximum occurs at  $\zeta = 1$ , yielding

$$\eta_{\max} = \frac{\pi}{8} \frac{a_0^2 \xi_0^3 \left( J'_N(k_{\perp}\rho_0) \right)^2 \beta_{\perp 0}^2}{(\gamma_0 - 1) \gamma_0 \sin \alpha} \exp\left(-\frac{1}{2}\right), \quad (12)$$

where  $\xi_0^2 = \xi^2(1 - n_z^2) = (\omega_0\gamma_0\omega/cu_{z0})^2$  is independent of  $\alpha$ . The small signal efficiency increases with decreasing angle  $\alpha$  (increasing index of

refraction  $n_z$ ) provided that  $\sin \alpha$  satisfies the inequality above Eq. (12). When  $\sin \alpha$  is too small, an exact solution of the cubic equation for  $\zeta$  is required and Eq. (12) is invalid.

We now calculate the start-up beam current using the small signal efficiency. Amplification of the electromagnetic radiation is possible if

$$\eta P_b > \frac{dE}{dt} = \frac{\omega}{Q} E, \quad (13)$$

where  $E = (1/4) \omega_0^2 L_R a_0^2 (\omega^2/c^2) (m^2 c^4 / |e|^2)$  is the total energy stored inside both resonators,  $L_R$  is the resonator length,  $dE/dt$  is the combined refraction, diffraction and transmission losses and  $Q$  is the quality factor for the cavity. Combining Eqs. (12) and (13) we obtain

$$I_s V_b > 2 \frac{\beta_{z0}^3}{\beta_{l0}^2} \frac{\gamma_0 (\gamma_0 - 1) \sin \alpha \exp(-\frac{1}{2})}{\pi [J'_N(k_{\perp} \rho_0)]^2} \frac{m^2 c^5 L_R}{|e|^2 \omega_0 Q}. \quad (14)$$

For small Larmor radius  $k_{\perp} \rho_0 \ll 1$  the start-up current  $I_s$  increases very quickly with the harmonic  $N$ ,  $I_s \propto 2^{2N} [(N-1)!]^2 / (k_{\perp} \rho_0)^{-(N-1)}$ . It is therefore desirable to operate at  $k_{\perp} \rho_0 \geq 1$  in order to have good coupling to the resonator modes and low start-up currents. In this case the start-up current scales roughly as the inverse maximum of the Bessel function derivative,  $I_s \propto N^{1/3}$ , increasing mildly with the harmonic  $N$ . We can achieve harmonic selection by choosing  $k_{\perp} \rho_0$  near a maximum of  $J'_N(k_{\perp} \rho_0)$  for the intended  $N$ th harmonic.

Expression (14) for the start-up current was derived using coherent resonator modes. These modes have evolved from an initial noise background of spontaneous cyclotron radiation. During the spontaneous emission stage preceding coherency most of the emitted radiation is contained within a cone of angle  $1/\gamma$  around the direction of the particle velocity  $v$ . Since  $v$  makes an angle  $\theta = \tan(v_{\perp}/v_z)$  with the magnetic field the condition  $|\theta - \alpha| \leq 1/\gamma$  must be met to avoid excessive losses during the start-up phase.

#### IV. THERMAL EFFECTS

One of the important features associated with the IREC maser is choosing the index of refraction appropriately to minimize the effects of the electron beam thermal spreads. Spreads in the initial electron momentum will cause a spread in the detuning parameters  $\Delta\omega_0$  among different particles. This in turn will cause an accelerated mixing in phase space opposing the nonlinear phase bunching and reducing in efficiency. According to Eq. (7) a standard deviation

$$\delta(\Delta\omega)_0 = \left[ \left( \frac{\partial \Delta\omega}{\partial \beta} \right)^2 \delta\beta_z^2 + \left( \frac{\partial \Delta\omega}{\partial \beta_1} \right)^2 \delta\beta_1^2 \right]^{1/2} = \left[ (\omega n_z - N\Omega_0 \gamma_0 \beta_{z0})^2 \delta\beta_z^2 + (N\Omega_0 \gamma_0 \beta_{10})^2 \delta\beta_1^2 \right]^{1/2} \quad (15)$$

in the initial detuning results from a beam distribution with velocity deviations  $\delta\beta_z$  and  $\delta\beta_1$ . The choice of resonator angle

$$n_z = \cos\alpha = \frac{N\Omega_0 \gamma_0 \beta_{z0}}{\omega} \quad (16)$$

causes the minimum initial spread in  $\Delta\omega_0$  for any beam thermal spreads. The minimum spread from Eqs. (15) and (16) can also be expressed in terms of the pitch angle spread  $\delta\theta_0$  and the energy spread  $\delta\gamma_0$ . Then, the requirement for small phase mixing among various particles over the interaction length  $L$ , namely  $\delta(\Delta\omega)_0 L / c\beta_z \ll \pi$ , suggests

$$\frac{\delta\theta_0}{\theta_0} + \frac{1}{\gamma_0^2} \frac{\delta\gamma_0}{\gamma_0} \ll \frac{\beta_{z0}}{2N_c (N\beta_{10}^2 \gamma_0^2)}, \quad (17)$$

where  $N_c = \Omega_0 L / (2\pi\gamma_0 c\beta_{z0})$  is the approximate number of cyclotron gyrations within the interaction length. The beam thermal spread requirements become more stringent with increasing harmonic  $N$ .

In the nonlinear operation regime the electrons get trapped in the wave potential<sup>14,38</sup> and execute synchrotron oscillations in phase space in a similar manner as in the conventional gyrotrons. The phase mixing among



various particles is now determined by the dependence of the trapped particle synchrotron period on the various parameters. The efficiency deterioration involves more factors than the initial spread in the detuning  $\Delta\omega_0$ , which is the dominant source of phase mixing only in the small signal regime  $a_0 \ll 1$ . Analytic predictions similar to Eq. (16) are hard to make in the nonlinear case. Our numerical results show that when the index of refraction is optimized according to (16) the nonlinear efficiency is practically insensitive to the energy spread  $\delta\gamma_0/\gamma_0$ .

## V. NUMERICAL RESULTS

In this section, we investigate various aspects of the nonlinear performance by numerically integrating Eqs. (6a) to (6e). We consider an electron beam of  $\gamma_0 = 2.5$  ( $\sim 0.75$  MeV) with  $\beta_{10} = 1/\gamma_0$  and  $\beta_{z0} = 0.825$  in a guide magnetic field of strength  $B_0 = 40$  kG. The appropriate index of refraction to minimize the effect of energy spread is, according to Eq. (16),  $n = 0.982$  which corresponds to an angle  $\alpha = 11^\circ$ . The frequency is upshifted by a factor  $N/(1 - n\beta_{z0}) = 5.26 N$  times the relativistic cyclotron frequency, and corresponds to a wavelength of 0.41 mm for the third harmonic  $N = 3$  and 0.31 mm for the fourth harmonic  $N = 4$ . The radiation spot size  $w_0$  is 0.50 cm and the Rayleigh lengths are 14.3 cm and 25.8 cm for  $N = 3$  and  $N = 4$  respectively. We consider a uniform guiding center distribution in the interval  $0 < k_{\perp} x_g < 2\pi$ .

Curves of efficiency  $\eta$  versus  $a_0$  for various values of the detuning  $\Delta\omega_0/\omega$  are plotted for  $N = 3$  and  $N = 4$  in Figs. 2 and 3 respectively. These results correspond to a cold beam without thermal spreads. We find the efficiency for the first few harmonic comparable to the efficiency for the fundamental<sup>29</sup> under the same operation parameters. Efficiency saturation occurs for larger amplitude  $a_0$  compared to the operation at the fundamental. Figure 4 shows the effects of finite beam quality on efficiency when the electron beam has either a spread in the pitch angle or a spread in energy. We plot the ratio of the thermalized efficiency  $\eta$  over the cold beam efficiency  $\eta_0$  for the third harmonic  $N = 3$  at fixed amplitude  $a_0 = 0.20$ . Curve (a) for zero energy spread,  $\Delta\gamma_0/\gamma_0 = 0$ , shows that the half width in the pitch angle spread that reduces efficiency by 50%, is equal to  $\Delta\theta_0/\theta_0 = 2\%$ . Curve (b) for zero pitch angle spread,  $\Delta\theta_0/\theta_0 = 0$ , shows that the half width in energy spread is  $\Delta\gamma_0/\gamma_0 = 13\%$ . Efficiency tends to be more sensitive on the spread in the pitch angle than the spread

in energies; therefore, we may simulate thermal effects by including only pitch angle spreads, cutting down on computing time.

Given that the large signal efficiency depends on few parameters, predictions about optimum operation at maximum efficiency are hard to make. One anticipates maximum efficiency when the transit time through the interaction regime is about equal to half the synchrotron period for a trapped particle. An optimum interaction length in the  $z$  direction  $L_z = 2L = 2w_0/\sin\alpha$  corresponds to a given synchrotron period  $\omega_b$ , which, in turn, depends on the five parameters  $a_0$ ,  $\gamma_0$ ,  $\theta_0$ ,  $\Delta\omega_0$  and  $\cos\alpha$ . This is illustrated in Fig. 5, which shows efficiency as a function of the traveled distance  $z$  for three different Gaussian profiles corresponding to different radiation spot sizes  $w_0$ , keeping the other parameters fixed. In curve (a) the interaction length is less than half the bounce distance  $L_b = \pi c \beta_z / \omega_b$  and the electrons exit the resonator before reaching the point of lowest energy in their trajectories. In curve (b) we have a good matching of  $L_z$  with  $L_b$  achieving the highest efficiency. In curve (c)  $L_z$  is larger than  $L_b$  and the electrons overshoot the point of minimum energy, gaining energy back from the wave and reducing efficiency.

From the practical point of view, one would like to optimize the design parameters of the resonator  $\alpha$  and  $L$  for a given beam energy  $\gamma_0$  and pitch angle  $\theta_0$  under the maximum energy load  $a_0^2$  sustained by the cavity. We already picked the operation angle  $\cos\alpha$  so as to minimize the effects of the beam energy spread. In Fig. 6 we show the efficiency as a function of the interaction length  $L_z$  by varying the spot size  $w_0$  and keeping all other parameters fixed. The upper curve shows the nonlinear efficiency for a monoenergetic electron beam of infinitesimal spot size  $b \ll w_0$ , and a uniform spread in the initial phase  $0 \leq \psi_0 \leq 2\pi$ . A uniform guiding center distribution  $0 \leq k_{\perp} x_g \leq 2\pi$  is included in the second curve. The resulting

efficiency reduction is no more than 30% indicating that some bunching in the guiding center position takes place as well. The addition of a 2% energy spread  $\delta\gamma_0/\gamma_0$  with zero pitch angle spread does not reduce efficiency considerably in the fourth curve. A 2% spread in the pitch angle  $\delta\theta_0/\theta_0$  with zero energy spread has a more pronounced effect on efficiency shown in the lowest curve (d). The overall picture shows that, for the parameters chosen, efficiency has a weak dependence on the interaction length  $L$  falling off slowly after an optimum length of  $L \sim 4$  cm.

#### ACKNOWLEDGMENT

This work was supported by the Department of Energy under Contract DE-AI05-83ER40117, Modification 3.

# REFERENCES

1. R. Q. Twiss, Aust. J. Phys. 11, 564 (1958).
2. A. V. Gaponov, Isv. Vyssh. Uchebn. Zaved, Radiofiz., 2, 450 (1959).
3. R. H. Pantell, Proc. IRE, 47, 1146 (1959).
4. J. Schneider, Phys. Rev. Lett. 2, 504 (1959).
5. J. L. Hirshfield and J. M. Wachtel, Phys. Rev. Lett. 12, 533 (1964).
6. A. V. Gaponov, M. I. Petelin and V. K. Yulpalov, Radio Phys. Quantum Electron. 10, 794 (1967).
7. V. L. Bratman, M. A. Moiseev, M. I. Petelin and R. E. Erm, Radio Phys. Quantum Electron. 16, 474 (1973).
8. D. V. Kisel, G. S. Korablev, V. G. Navel'yev, M. I. Petelin and Sh. E. Tsimring, Radio Eng. Electron. Phys. 19, No. 4, 95 (1974).
9. N. I. Zaytsev, T. B. Pankratova, M. I. Petelin and V. A. Flyagin, Radio Eng. Electron. Phys. 19, No. 5, 103 (1974).
10. V. L. Granatstein, M. Herndon, R. K. Parker and P. Sprangle, IEEE J. Quantum Electron. QE-10 No. 9, p. 651 (1974).
11. E. Ott and W. M. Manheimer, IEEE Trans. Plasma Science PS-3, 1 (1975).
12. V. L. Granatstein, P. Sprangle, M. Herndon and R. K. Parker, J. Appl. Phys. 46, 2021 (1975).
13. P. Sprangle and W. M. Manheimer, Phys. Fluids 18, 224 (1975).
14. P. Sprangle and A. T. Drobot, IEEE Trans. Microwave Theory and Techniques MTT-25, 528 (1977).
15. J. L. Hirshfield and V. L. Granatstein, IEEE Trans. Microwave Theory and Tech. MTT-25, 522 (1977).
16. K. R. Chu and J. L. Hirshfield, Phys. Fluids 21, 461 (1978).
17. V. L. Bratman, N. S. Ginzburg and M. I. Petelin, Optics Commun. 30, 409 (1979).
18. P. Sprangle and R. A. Smith, J. Appl. Phys. 51, 6, p. 3001 (1980).

19. C. S. Wu and L. C. Lee, *Astrophys. J.* 230, 621 (1979).
20. P. L. Pritchett, *Phys. Fluids* 29, 2919 (1986).
21. A. Bondeson, W. M. Manheimer and E. Ott, *Infrared and Millimeter Waves* 9, 309 (1983).
22. P. Sprangle, J. L. Vomvorides and W. M. Manheimer, *Appl. Phys. Lett.* 38, 310 (1981); also *Phys. Rev.* A23, 3127 (1981).
23. J. L. Vomvorides and P. Sprangle, *Phys. Rev.* A25, 931 (1982).
24. M. I. Petelin, *Radiophysics and Quant. Electron.* 17, 686 (1974); also V. L. Bratman, N. S. Ginzburg and M. I. Petelin, *Optics Commun.* 30, 409 (1979).
25. V. L. Bratman, G. G. Denisov, N. S. Ginzburg and M. I. Petelin, *IEEE J. Quantum Electronics* QE-19, 282 (1983).
26. K. E. Kreisher and R. J. Temkin, *Infrared and Millimeter Waves*, 7, 377 (1983).
27. A. W. Fliflet, *Intl. J. Electron.* 61, 1049 (1986).
28. P. Sprangle, C. M. Tang and P. Serafim, *Nucl. Instr. and Methods in Phys.* A250, 361 (1986).
29. P. Sprangle, C. M. Tang and P. Serafim, *Appl. Phys. Lett.* 49, 1154 (1986).
30. S. Riyopoulos, C. M. Tang and P. Sprangle, *Phys. Rev.* A36, xxxx (1987)
31. C. M. Tang, S. Riyopoulos and P. Sprangle, *Proc. Eighth Intl. Conf. on Free Electron Lasers, Glasgow, Scotland, (North Holland, ed. M. Poole) pg. xxx, 1986.*
32. V. L. Bratman, N. S. Ginzburg and A. S. Sergeev, *Sov. Phys. JETP* 55, 479 (1985).
33. A. V. Gaponov, V. A. Flyagin, A. L. Goldenberg, G. S. Nusinovich, Sh. E. Tsimring, V. G. Usov and S. N. Vlasov, *Intl. J. Electron.* 51, 277 (1981).

34. B. G. Danly and R. J. Temkin, Phys. Fluids 29, 561 (1985).
35. B. Levush, A. Bondeson, W. M. Manheimer and E. Ott, Intl. J. Electron. 54, 749 (1983).
36. B. Levush and W. Manheimer, IEEE Trans. of Microwave Th. and Techn. MTT-32, 1398 (1984)
37. Y. Gell, J. R. Torstensson, H. Wilhelmsson and B. Levush, Appl. Phys. B27, 15 (1982)
38. J. L. Vomvorides, Intl. J. Electron. 53, 555 (1982).

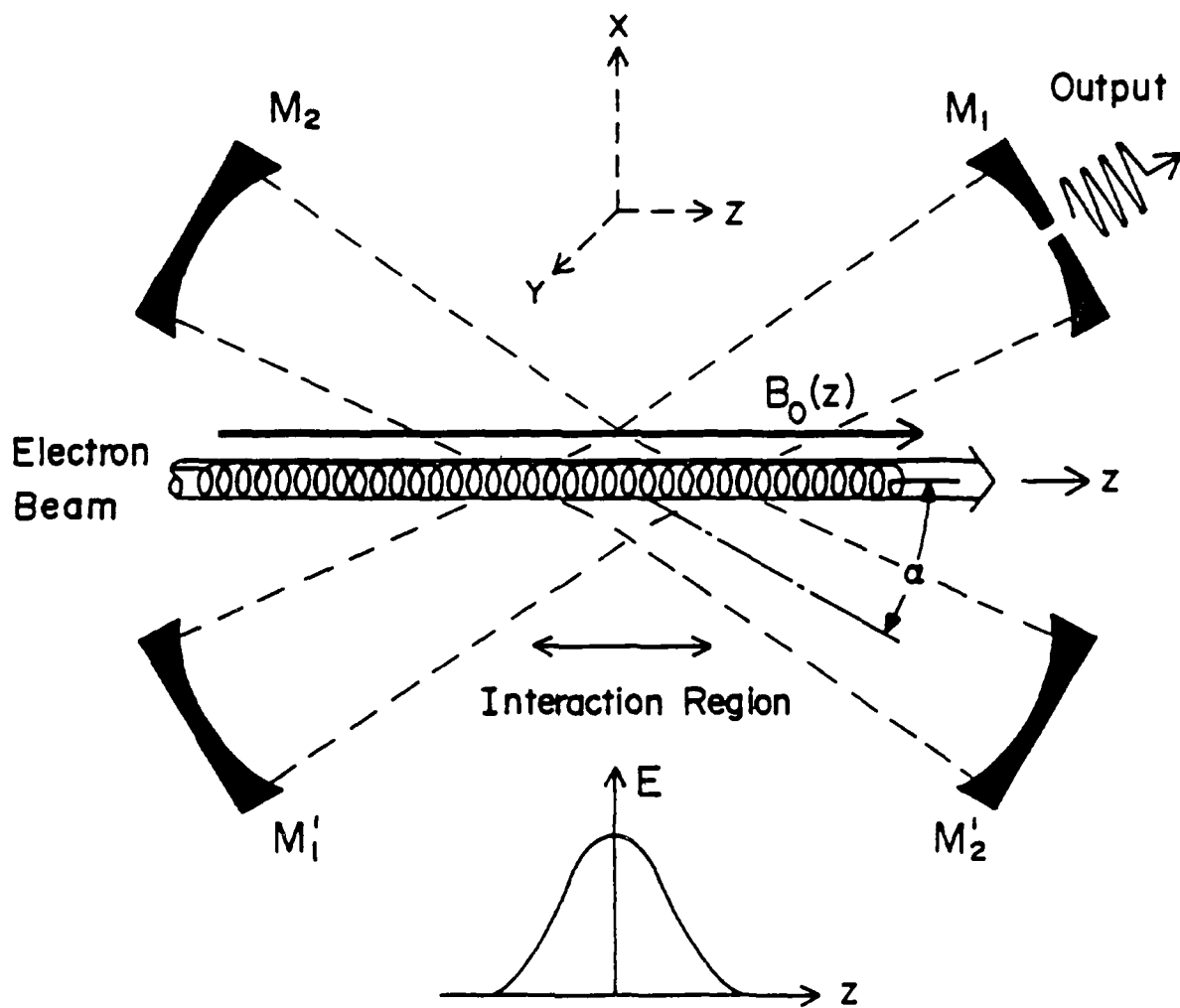


Figure 1. Schematic illustration of the Induced Resonance Electron Cyclotron Maser.



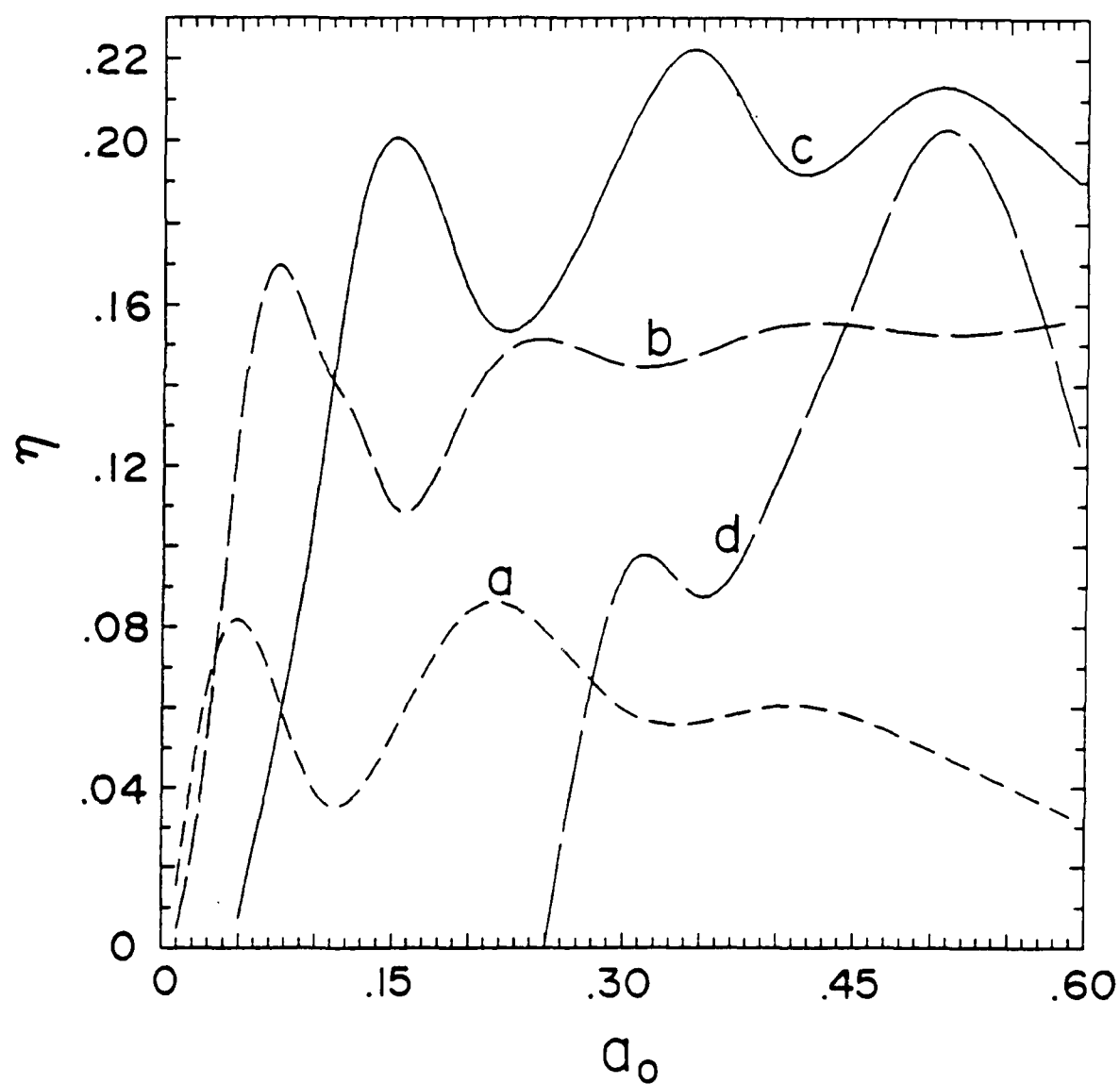


Figure 2. Plots of efficiency  $\eta$  versus the normalized radiation amplitude  $a_0$  at the third harmonic  $N = 3$  and for detuning parameters  $\Delta\omega_0/\omega$  equal to (a). 0.025 (b). 0.050 (c). 0.075 and (d). 0.100 respectively. A cold beam of uniform guiding center spread is considered. The simulation parameters are  $r_0 = 2.5$ ,  $\alpha = 11^\circ$ ,  $w_0 = 0.5$  cm and  $\theta_0 = 0.48$ .

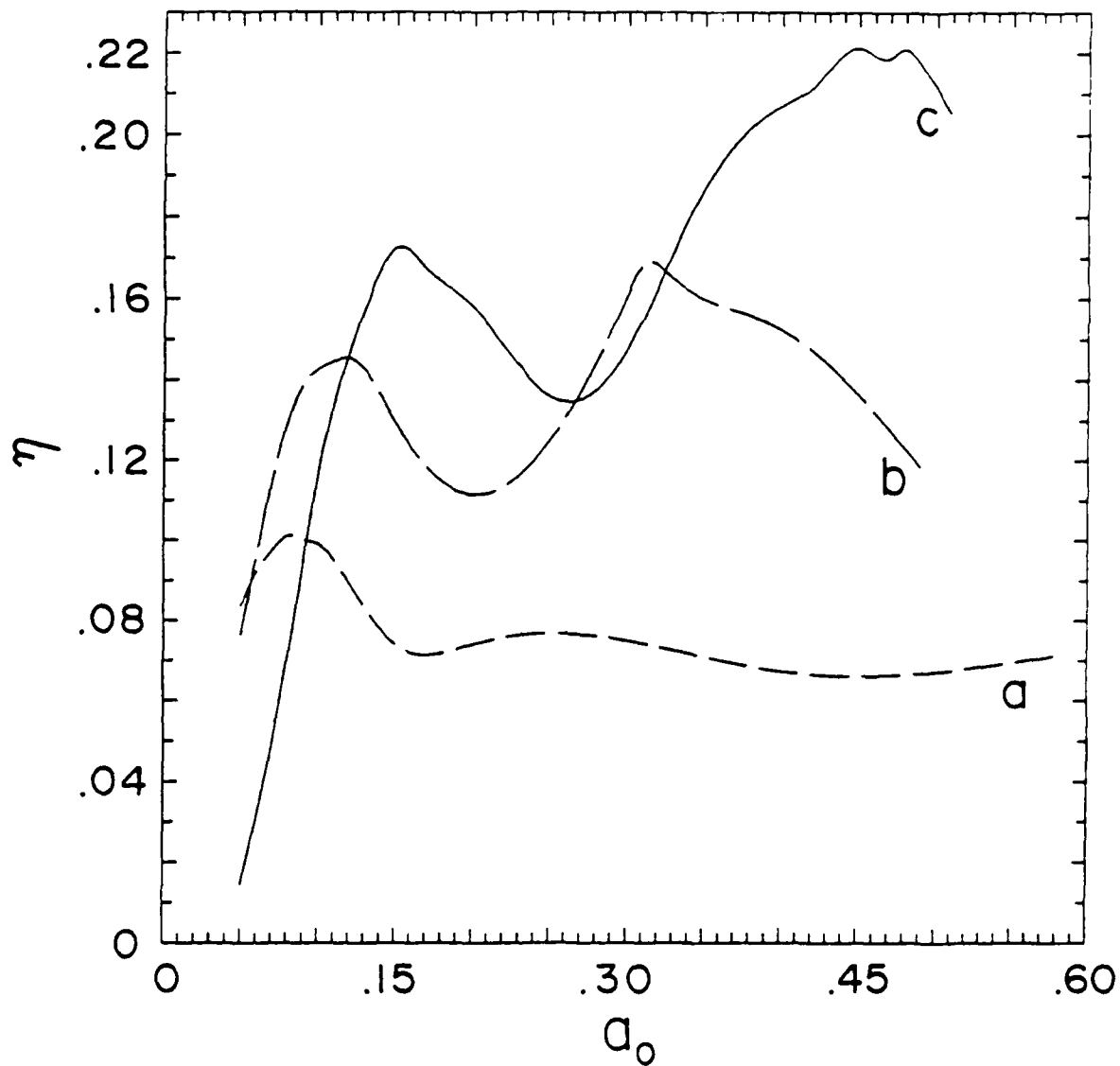


Figure 3. Plots of efficiency  $\eta$  versus the normalized radiation amplitude  $a_0$  at the fourth harmonic  $N = 4$  for detuning parameter  $\Delta\omega_0/\omega$  equal to (a). 0.025 (b) 0.037 and (c) 0.050 respectively. The other parameters are the same as in Fig. 2.

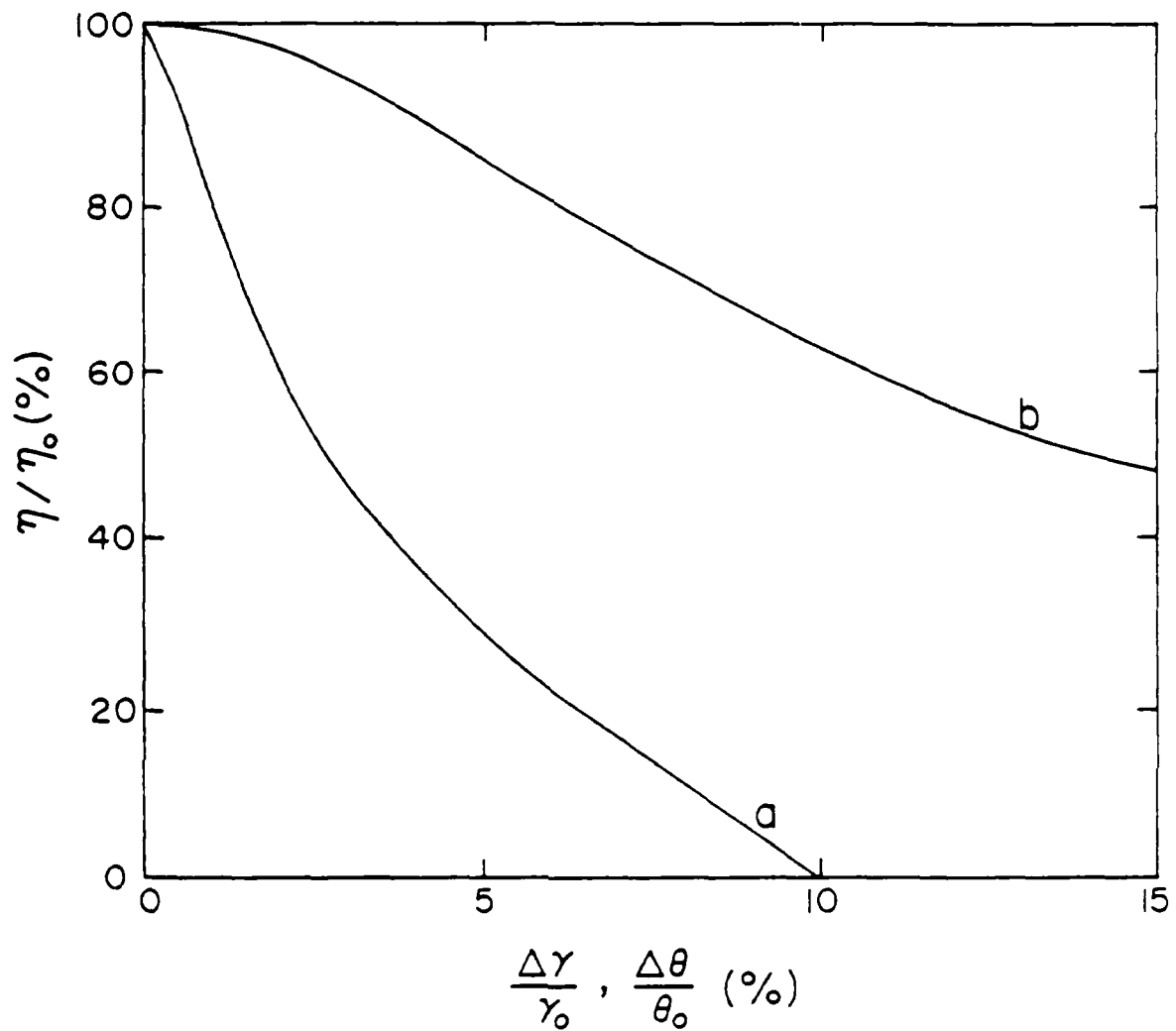


Figure 4. Dependence of the efficiency on beam thermal spreads. Shown is the ratio of thermalized to cold beam efficiency  $\eta/\eta_0$  as a function of (a) pitch angle spread  $\delta\theta_0/\theta_0$  with  $\delta\gamma_0 = 0$  and (b) energy spread  $\delta\gamma_0/\gamma_0$  with  $\delta\theta_0 = 0$ . The parameters are the same as in Fig. 2 with  $\Delta\omega_0/\omega = 0.075$ .

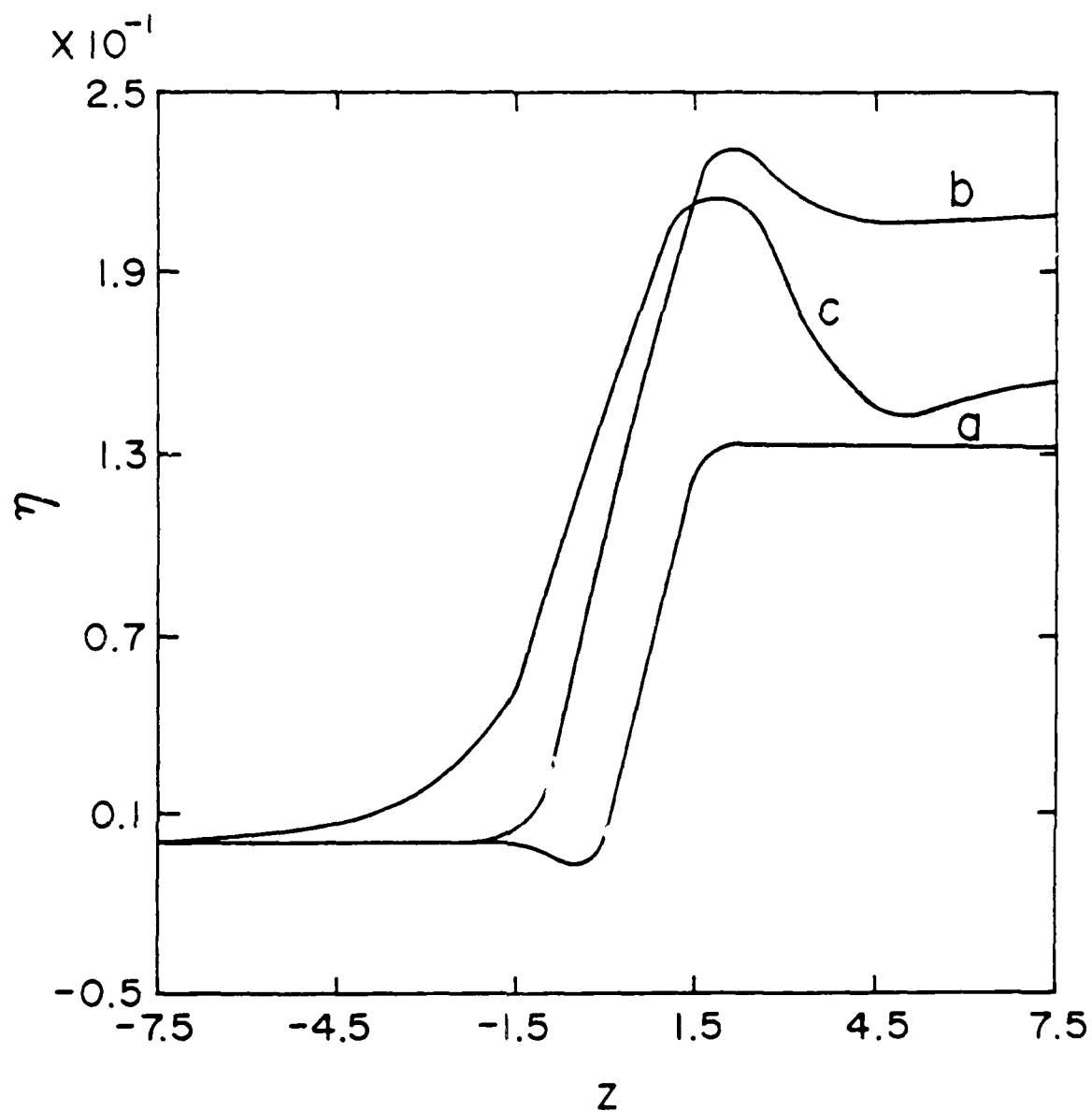


Figure 5. Plots of efficiency  $\eta$  versus travelled distance  $z$  inside the resonator for various interaction lengths corresponding to different radiation spot sizes  $w_0$ . The center of the resonator is at  $z = 0$ .  $L_z$  is equal to (a) 2.64 cm (b) 4.24 cm and (c) 7.41 cm. The parameters are the same as in Fig. 2 with  $\Delta\omega_0/\omega = 0.075$ .

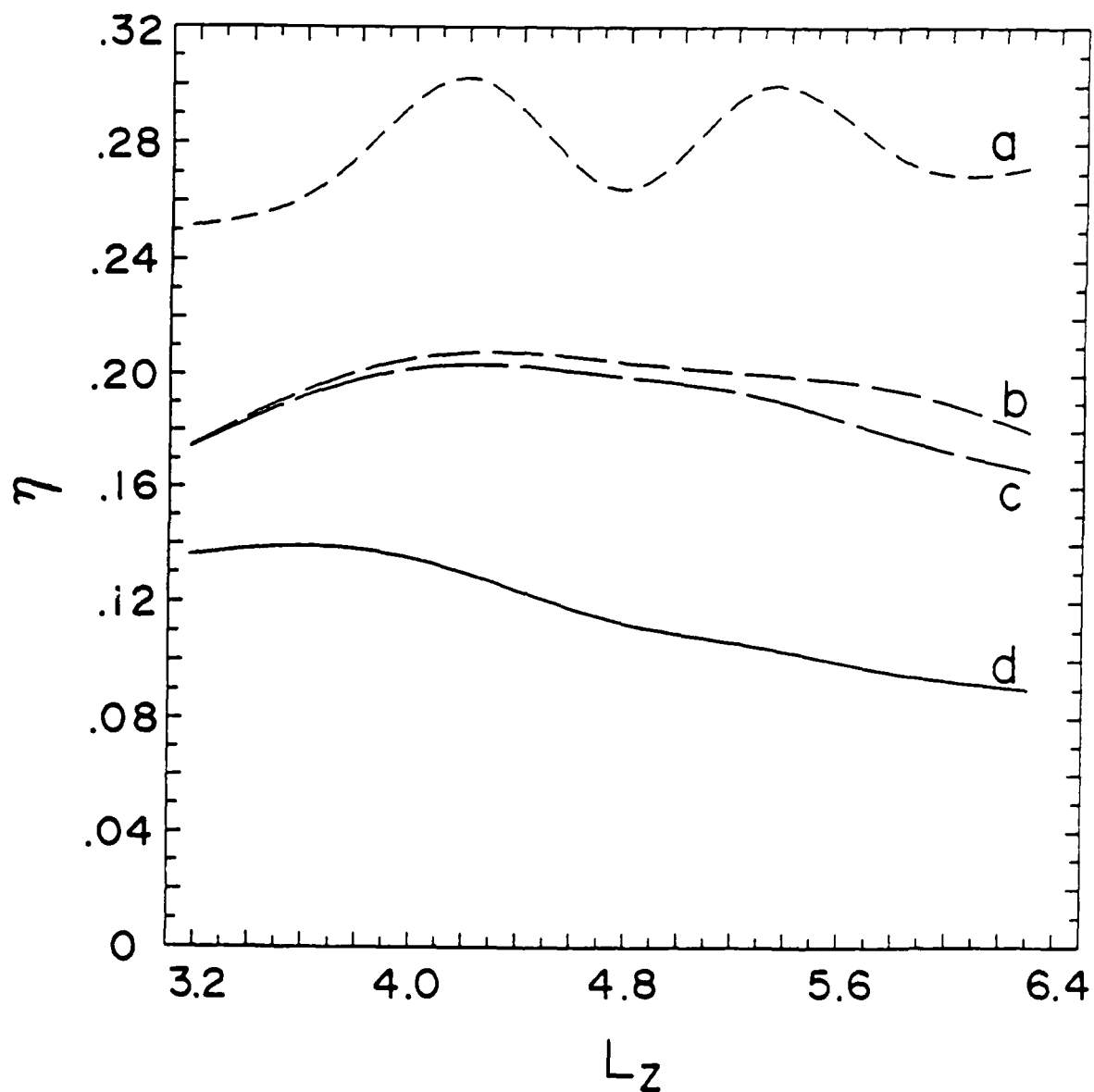


Figure 6. Plots of efficiency  $\eta$  versus interaction length  $L_z$  with the same parameters as before. Curve (a) is for a cold beam of zero cross section and curves (b)-(d) for a uniform guiding center spread with (b) no thermal spreads (c) 2% energy spread and (d) 2% pitch angle spread.

DISTRIBUTION LIST\*

Naval Research Laboratory  
4555 Overlook Avenue, S.W.  
Washington, DC 20375-5000

Attn: Code 1000 - CAPT William C. Miller  
1001 - Dr. T. Coffey  
4603 - Dr. W.W. Zachary  
4700 - Dr. S. Ossakow (26 copies)  
4710 - Dr. C.A. Kapetanakos  
4730 - Dr. R. Elton  
4740 - Dr. W.M. Manheimer  
4740 - Dr. S. Gold  
4790 - Dr. P. Sprangle (100 copies)  
4790 - Dr. C.M. Tang (50 copies)  
4790 - Dr. M. Lampe ''  
4790 - Dr. Y.Y. Lau  
4790A- W. Brizzi  
6652 - Dr. N. Seeman  
6840 - Dr. S.Y. Ahn  
6840 - Dr. A. Ganguly  
6840 - Dr. R.K. Parker  
6850 - Dr. L.R. Whicker  
6875 - Dr. R. Wagner  
2628 - Documents (20 copies)  
2634 - D. Wilbanks, 4  
1220 - 1 copy

\* Every name listed on distribution gets one copy except for those where extra copies are noted.

Dr. R. E. Aamodt  
Science Applications Intl. Corp.  
1515 Walnut Street  
Boulder, CO 80302

Dr. B. Amini  
1763 B. H.  
U. C. L. A.  
Los Angeles, CA 90024

Dr. D. Bach  
Los Alamos National Laboratory  
P. O. Box 1663  
Los Alamos, NM 87545

Dr. D. C. Barnes  
Science Applications Intl. Corp.  
Austin, TX 78746

Dr. L. R. Barnett  
3053 Merrill Eng. Bldg.  
University of Utah  
Salt Lake City, UT 84112

Dr. S. H. Batha  
Lab. for Laser Energetics &  
Dept. of Mech. Eng.  
Univ. of Rochester  
Rochester, NY 14627

Dr. F. Bauer  
Courant Inst. of Math. Sciences  
New York University  
New York, NY 10012

Dr. Peter Baum  
General Research Corp.  
P. O. Box 6770  
Santa Barbara, CA 93160

Dr. Russ Berger  
FL-10  
University of Washington  
Seattle, WA 98185

Dr. O. Betancourt  
Courant Inst. of Math. Sciences  
New York University  
New York, NY 10012

Dr. B. Bezzerides  
MS-E531  
Los Alamos National Laboratory  
P. O. Box 1663  
Los Alamos, NM 87545

Dr. Irving J. Bigio  
Lawrence Livermore National Laboratory  
P. O. Box 808, L-626  
Livermore, CA 91550

Dr. Leroy N. Blumberg  
U.S. Dept. of Energy  
Division of High Energy Physics  
ER-224/Germantown  
Wash., DC 20545

Dr. Mario Bosco  
University of California, Santa Barbara  
Santa Barbara, CA 93106

Dr. Howard E. Brandt  
Department of the Army  
Harry Diamond Laboratory  
2800 Powder Mill Road  
Adelphi, MD 20783

Dr. Richard J. Briggs  
Lawrence Livermore National Laboratory  
P. O. Box 808, L-626  
Livermore, CA 91550

Dr. Bob Brooks  
FL-10  
University of Washington  
Seattle, WA 98195

Dr. Paul J. Channell  
AT-6, MS-H818  
Los Alamos National Laboratory  
P. O. Box 1663  
Los Alamos, NM 87545

Dr. A. W. Chao  
Stanford Linear Accelerator Center  
Stanford University  
Stanford, CA 94305

Dr. Francis F. Chen  
UCLA, 7731 Boelter Hall  
Electrical Engineering Dept.  
Los Angeles, CA 90024

Dr. K. Wendell Chen  
Center for Accel. Tech.  
University of Texas  
P.O. Box 19363  
Arlington, TX 76019

Dr. Pisin Chen  
SLAC, Bin 26  
P.O. Box 4349  
Stanford, CA 94305

Dr. Marvin Chodorow  
Stanford University  
Dept. of Applied Physics  
Stanford, CA 94305

Major Bart Clare  
USASDC  
P. O. Box 15280  
Arlington, VA 22215-0500

Dr. Christopher Clayton  
UCLA, 1538 Boelter Hall  
Electrical Engineering Dept.  
Los Angeles, CA 90024

Dr. David Cline  
Dept. of Physics  
University of Wisconsin  
Madison, WI 53706

Dr. Bruce I. Cohen  
Lawrence Livermore National Laboratory  
P. O. Box 808  
Livermore, CA 94550

Dr. B. Cohn  
L-630  
Lawrence Livermore National Laboratory  
P. O. Box 808  
Livermore, CA 94550

Dr. B. Cole  
Univ. of Wisconsin  
Madison, WI 53706

Dr. Francis T. Cole  
Fermi National Accelerator Laboratory  
Physics Section  
P. O. Box 500  
Batavia, IL 60510

Dr. Richard Cooper  
Los Alamos National Laboratory  
P. O. Box 1663  
Los Alamos, NM 87545

Dr. Ernest D. Courant  
Brookhaven National Laboratory  
Upton, NY 11973

Dr. Paul L. Csonka  
Institute of Theoretical Sciences  
and Department of Physics  
University of Oregon  
Eugene, Oregon 97403

Mr. Chris Darrow  
UCLA  
1-130 Knudsen Hall  
Los Angeles, CA 90024

Dr. J. M. Dawson  
Department of Physics  
University of California, Los Angeles  
Los Angeles, CA 90024

Dr. A. Dimos  
NW16-225  
M. I. T.  
Cambridge, MA 02139

Dr. J. E. Drummond  
Western Research Corporation  
8616 Commerce Ave  
San Diego, CA 92121

Dr. Adam Drobot  
Science Applications Intl. Corp.  
1710 Goodridge Dr.  
Mail Stop G-8-1  
McLean, VA 22102

Dr. D. F. DuBois, T-DOT  
Los Alamos National Laboratory  
Los Alamos, NM 87545

Dr. J. J. Ewing  
Spectra Technology  
2755 Northup Way  
Bellevue, WA 98004

Dr. Frank S. Felber  
11011 Torreyana Road  
San Diego, CA 92121

Dr. Richard C. Fernow  
Brookhaven National Laboratory  
Upton, NY 11973

Dr. H. Figueroa  
1-130 Knudsen Hall  
U. C. L. A.  
Los Angeles, CA 90024



Dr. Jorge Fontana  
Elec. and Computer Eng. Dept.  
Univ. of Calif. at Santa Barbara  
Santa Barbara, CA 93106

Dr. David Forslund  
Los Alamos National Laboratory  
P. O. Box 1663  
Los Alamos, NM 87545

Dr. John S. Fraser  
Los Alamos National Laboratory  
P.O. Box 1663, MS H825  
Los Alamos, NM 87545

Dr. P. Garabedian  
Courant Inst. of Math. Sciences  
New York University  
New York, NY 10012

Dr. Walter Gekelman  
UCLA - Dept. of Physics  
1-130 Knudsen Hall  
Los Angeles, CA 90024

Dr. Dennis Gill  
Los Alamos National Laboratory  
P. O. Box 1663  
Los Alamos, NM 87545

Dr. B. B. Godfrey  
Mission Research Corporation  
1720 Randolph Road, SE  
Albuquerque, NM 87106

Dr. P. Goldston  
Los Alamos National Laboratory  
P. O. Box 1663  
Los Alamos, NM 87545

Prof. Louis Hand  
Dept. of Physics  
Cornell University  
Ithaca, NY 14853

Dr. J. Hays  
TRW  
One Space Park  
Redondo Beach, CA 90278

Dr. Wendell Horton  
University of Texas  
Physics Dept., RLM 11.320  
Austin, TX 78712

Dr. J. Y. Hsu  
General Atomic  
San Diego, CA 92138

Dr. H. Huey  
Varian Associates  
B-118  
611 Hansen Way  
Palo Alto, CA 95014

Dr. Robert A. Jameson  
Los Alamos National Laboratory  
AT-Division, MS H811  
P.O. Box 1663  
Los Alamos, NM 87545

Dr. G. L. Johnston  
NW16-232  
M. I. T.  
Cambridge, MA 02139

Dr. Shayne Johnston  
Physics Department  
Jackson State University  
Jackson, MS 39217

Dr. Mike Jones  
MS B259  
Los Alamos National Laboratory  
P. O. Box 1663  
Los Alamos, NM 87545

Dr. C. Joshi  
7620 Boelter Hall  
Electrical Engineering Department  
University of California, Los Angeles  
Los Angeles, CA 90024

Dr. E. L. Kane  
Science Applications Intl. Corp.  
McLean, VA 22102

Dr. Tom Katsouleas  
UCLA, 1-130 Knudsen Hall  
Department of Physics  
Los Angeles, CA 90024

Dr. Rhon Keinigs MS-259  
Los Alamos National Laboratory  
P. O. Box 1663  
Los Alamos, NM 87545

Dr. Kwang-Je Kim  
Lawrence Berkeley Laboratory  
University of California, Berkeley  
Berkeley, CA 94720

Dr. S. H. Kim  
Center for Accelerator Technology  
University of Texas  
P.O. Box 19363  
Arlington, TX 76019

Dr. Joe Kindel  
Los Alamos National Laboratory  
P. O. Box 1663, MS E531  
Los Alamos, NM 87545

Dr. Ed Knapp  
Los Alamos National Laboratory  
P. O. Box 1663  
Los Alamos, NM 87545

Dr. Peter Kneisel  
Cornell University  
F. R. Newman Lab. of Nucl. Studies  
Ithaca, NY 14853

Dr. Norman M. Kroll  
University of California, San Diego  
San Diego, CA 92093

Dr. Kenneth Lee  
Los Alamos National Laboratory  
P.O. Box 1663, MS E531  
Los Alamos, NM 87545

Dr. N. C. Luhmann, Jr.  
7702 Boelter Hall  
U. C. L. A.  
Los Angeles, CA 90024

Dr. K. Maffee  
University of Maryland  
E. R. B.  
College Park, MD 20742

Dr. B. D. McDaniel  
Cornell University  
Ithaca, NY 14853

Dr. Colin McKinstrie  
Los Alamos National Laboratory  
P. O. Box 1663  
Los Alamos, NM 87545

Dr. A. Mondelli  
Science Applications Intl. Corp.  
1710 Goodridge Drive  
McLean, VA 22101

Dr. Warren Mori  
1-130 Knudsen Hall  
U. C. L. A.  
Los Angeles, CA 90024

Dr. P. L. Morton  
Stanford Linear Accelerator Center  
P. O. Box 4349  
Stanford, CA 94305

Dr. John A. Nation  
Laboratory of Plasma Studies  
369 Upson Hall  
Cornell University  
Ithaca, NY 14853

Dr. K. C. Ng  
Courant Inst. of Math. Sciences  
New York University  
New York, NY 10012

Dr. Robert J. Noble  
S.L.A.C., Bin 26  
Stanford University  
P.O. Box 4349  
Stanford, CA 94305

Dr. J. Norem  
Argonne National Laboratory  
Argonne, IL 60439

Dr. Craig L. Olson  
Sandia National Laboratories  
Plasma Theory Division 1241  
P.O. Box 5800  
Albuquerque, NM 87185

Dr. H. Oona  
MS-E554  
Los Alamos National Laboratory  
P. O. Box 1663  
Los Alamos, NM 87545

Dr. Robert B. Palmer  
Brookhaven National Laboratory  
Upton, NY 11973

Dr. Richard Pantell  
Stanford University  
308 McCullough Bldg.  
Stanford, CA 94305

Dr. John Pasour  
Mission Research Corporation  
5503 Cherokee Ave.  
Suite 201  
Alexandria, VA 22312

Dr. Samuel Penner  
Center for Radiation Research  
National Bureau of Standards  
Gaithersburg, MD 20899

Dr. Claudio Pellegrini  
National Synchrotron Light Source  
Brookhaven National Laboratory  
Upton, NY 11973

Dr. Melvin A. Piestrup  
Adelphi Technology  
13800 Skyline Blvd. No. 2  
Woodside, CA 94062

Dr. Z. Pietrzyk  
FL-10  
University of Washington  
Seattle, WA 98185

Dr. Don Prosnitz  
Lawrence Livermore National Laboratory  
P. O. Box 808  
Livermore, CA 94550

Dr. R. Ratovsky  
Physics Department  
University of California at Berkeley  
Berkeley, CA 94720

Dr. Charles W. Roberson  
Office of Naval Research  
Detachment Arlington  
800 North Quincy St., BCT # 1  
Arlington, VA 22217-5000

Dr. Stephen Rockwood  
Los Alamos National Laboratory  
P. O. Box 1663  
Los Alamos, NM 87545

Dr. Harvey A. Rose, T-DOT  
Los Alamos National Laboratory  
Los Alamos, NM 87545

Dr. James B. Rosenzweig  
Dept. of Physics  
University of Wisconsin  
Madison, WI 53706

Dr. Alessandro G. Ruggiero  
Argonne National Laboratory  
Argonne, IL 60439

Dr. R. D. Ruth  
SLAC, Bin 26  
P. O. Box 4349  
Stanford, CA 94305

Dr. Jack Sandweiss  
Gibbs Physics Laboratory  
Yale University  
260 Whitney Avenue  
P. O. Box 6666  
New Haven, CT 06511

Dr. Al Saxman  
Los Alamos National Laboratory  
P.O. Box 1663, MS E523  
Los Alamos, NM 87545

Dr. George Schmidt  
Stevens Institute of Technology  
Department of Physics  
Hoboken, NJ 07030

Dr. N. C. Schoen  
TRW  
One Space Park  
Redondo Beach, CA 90278

Dr. Frank Selph  
U. S. Department of Energy  
Division of High Energy Physics, ER-224  
Washington, DC 20545

Dr. Andrew M. Sessler  
Lawrence Berkeley Laboratory  
University of California, Berkeley  
Berkeley, CA 94720

Dr. Richard L. Sheffield  
Los Alamos National Laboratory  
P.O. Box 1663, MS H825  
Los Alamos, NM 87545

Dr. John Siambis  
Lockheed Palo Alto Research Laboratory  
3251 Hanover Street  
Palo Alto, CA 94304

Dr. Robert Siemann  
Dept. of Physics  
Cornell University  
Ithaca, NY 14853

Dr. J. D. Simpson  
Argonne National Laboratory  
Argonne, IL 60439

Dr. Charles K. Sinclair  
Stanford University  
P. O. Box 4349  
Stanford, CA 94305

Dr. Sidney Singer  
MS-E530  
Los Alamos National Laboratory  
P. O. Box 1663  
Los Alamos, NM 87545

Dr. R. Siusher  
AT&T Bell Laboratories  
Murray Hill, NJ 07974

Dr. Jack Slater  
Mathematical Sciences, NW  
2755 Northup Way  
Bellevue, WA 98009

Dr. Todd Smith  
Hansen Laboratory  
Stanford University  
Stanford, CA 94305

Dr. Richard Spitzer  
Stanford Linear Accelerator Center  
P. O. Box 4347  
Stanford, CA 94305

Mr. J. J. Su  
UCLA  
1-130 Knudsen Hall  
Los Angeles, CA 90024

Prof. Ravi Sudan  
Electrical Engineering Department  
Cornell University  
Ithaca, NY 14853

Dr. Don J. Sullivan  
Mission Research Corporation  
1720 Randolph Road, SE  
Albuquerque, NM 87106

Dr. David F. Sutter  
U. S. Department of Energy  
Division of High Energy Physics, ER-224  
Washington, DC 20545

Dr. T. Tajima  
Department of Physics  
and Institute for Fusion Studies  
University of Texas  
Austin, TX 78712

Dr. Lee Teng, Chairman  
Fermilab  
P.O. Box 500  
Batavia, IL 60510

Dr. H. S. Uhm  
NSWC  
White Oak Laboratory  
Silver Spring, MD 20903-5000

U. S. Naval Academy (2 copies)  
Director of Research  
Annapolis, MD 21402

Dr. William A. Wallenmeyer  
U. S. Dept. of Energy  
High Energy Physics Div., ER-22  
Washington, DC 20545

Dr. John E. Walsh  
Department of Physics  
Dartmouth College  
Hanover, NH 03755

Dr. Tom Wangler  
Los Alamos National Laboratory  
P. O. Box 1663  
Los Alamos, NM 87545

Dr. S. Wilks  
Physics Dept.  
1-130 Knudsen Hall  
UCLA  
Los Angeles, CA 90024

Dr. Perry B. Wilson  
Stanford Linear Accelerator Center  
Stanford University  
P.O. Box 4349  
Stanford, CA 94305

Dr. W. Woo  
Applied Science Department  
University of California at Davis  
Davis, CA 95616

Dr. Jonathan Wurtele  
M.I.T.  
NW 16-234  
Plasma Fusion Center  
Cambridge, MA 02139

Dr. Yi-Ton Yan  
Los Alamos National Laboratory  
MS-K764  
Los Alamos, NM 87545

Dr. M. Yates  
Los Alamos National Laboratory  
P. O. Box 1663  
Los Alamos, NM 87545

Dr. Ken Yoshioka  
Laboratory for Plasma and Fusion  
University of Maryland  
College Park, MD 20742

Dr. R. W. Ziolkowski, L-156  
Lawrence Livermore National Laboratory  
P. O. Box 808  
Livermore, CA 94550

END

12-87

DTIC